


## Thiuram disulfide intercalated hybrid materials of layered lead and cadmium iodides

K. Ramalingam & A. Ilakkiya

To cite this article: K. Ramalingam & A. Ilakkiya (2016): Thiuram disulfide intercalated hybrid materials of layered lead and cadmium iodides, Phosphorus, Sulfur, and Silicon and the Related Elements, DOI: [10.1080/10426507.2015.1073280](https://doi.org/10.1080/10426507.2015.1073280)

To link to this article: <http://dx.doi.org/10.1080/10426507.2015.1073280>

 View supplementary material 

 Published online: 23 Mar 2016.

 Submit your article to this journal 

 Article views: 3

 View related articles 

 View Crossmark data 

## Thiuram disulfide intercalated hybrid materials of layered lead and cadmium iodides

K. Ramalingam and A. Ilakkiya

Department of Chemistry, Annamalai University, Annamalainagar, Tamil Nadu, India

### ABSTRACT

Thiuram disulfide intercalates of lead(II) and cadmium(II) were prepared by the reaction of binary layered metal iodides with five dithiocarbamates in air. The intercalates were characterized by elemental analysis, Powder X-ray diffraction (XRD), infrared (IR), ultraviolet–visible spectroscopy, diffuse reflectance spectroscopy, scanning electron microscopy (SEM), energy dispersive X-ray spectroscopy, high-resolution transmission electron microscopy (HRTEM), and atomic force microscopy (AFM) techniques. IR showed increased contribution of the thioureide bond and the presence of weak disulfide stretching frequency. Powder XRD showed the characteristic intermediate  $2\theta$  signal confirming the intercalation. Powder XRD clearly differentiated intercalates from the iodinated product of dithiocarbamate. As the bulkiness of substituents on disulfide increased, “d” also increased. The higher thermal stability associated with intercalates clearly suggests a strong ionic interaction and a difficult de-intercalation. SEM images of lead intercalates indicated crystalline nature. The intercalates appeared as rods or spheres. The diallyl-intercalate,  $[\text{PbI}_2](\text{H}_5\text{C}_3)_2\text{NCSS-SSCN}(\text{C}_3\text{H}_5)_2$  (where  $(\text{H}_5\text{C}_3)_2\text{NCSS-SSCN}(\text{C}_3\text{H}_5)_2$  is diallylthiuram disulfide), shows “net like structures.” Intercalation of oxidized dithiocarbamates in the “galleries” of layered  $\text{PbI}_2/\text{CdI}_2$  is observed. HRTEM and AFM analysis of intercalates showed the particles to be nano-rods.

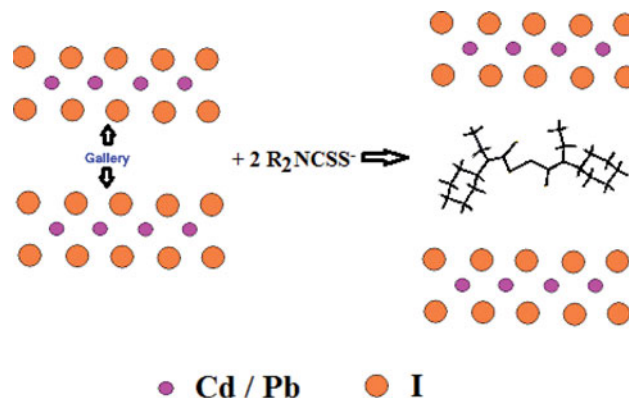
### ARTICLE HISTORY

Received 22 May 2015  
Accepted 13 July 2015

### KEYWORDS

Layered iodides;  
intercalation; thiuram  
disulfide; powder XRD; SEM;  
HRTEM

### GRAPHICAL ABSTRACT



### Introduction

Hybrid materials refer to a wide variety of materials such as ordered crystalline coordination polymers, amorphous sol-gel compounds, and a combination of organic and inorganic units with or without interactions.<sup>1–3</sup> Interest in these compounds has seen a spurt in recent times due to reports of the use of hybrid perovskites in solar cells.<sup>4–8</sup> The most important advantage of hybrid materials is the favorable combination of the properties of organic and inorganic components, as layered hybrid compounds are an important class of materials that find extensive applications in devices.<sup>9–14</sup> Layered cadmium(II) and lead(II) are wide band gap semiconductors,<sup>15</sup> their potential use as X-ray detectors, holographic data recorders, and as solar cell materials

in the visible range have been investigated.<sup>16</sup> Hybrid materials involving lead iodide ( $\text{PbI}_2$ ) and amines investigated by photoluminescence, infrared absorption, and Raman spectroscopy revealed different properties for the hybrid material in comparison with those of pure  $\text{PbI}_2$  and amine.<sup>17–20</sup> Polymer-embedded  $\text{PbI}_2$  materials are thermally stable and are transparent to light and find applications in many fields.<sup>21</sup> Structurally, the heavy metal iodides are similar to the transition metal dichalcogenides and their electronic structures are similar to the graphite.<sup>22,23</sup> Heavy metal iodides have a plane of hexagonally packed heavy metal atoms sandwiched between two planes of hexagonally packed iodine atoms as depicted in Figure 1. Each layer of such a triple-plane sandwich has an I–M–I sequence, where “I” represents the iodine atoms and “M” represents the heavy metal

**CONTACT** K. Ramalingam  [krauchem@yahoo.com](mailto:krauchem@yahoo.com)  Department of Chemistry, Annamalai University, Annamalainagar 608 002, Tamil Nadu, India.

Color versions of one or more of the figures in the article can be found online at [www.tandfonline.com/gps](http://www.tandfonline.com/gps).

Supplemental data for this article can be accessed on the publisher's website at <http://dx.doi.org/10.1080/10426507.2015.1073280>

© 2016 Taylor & Francis Group, LLC

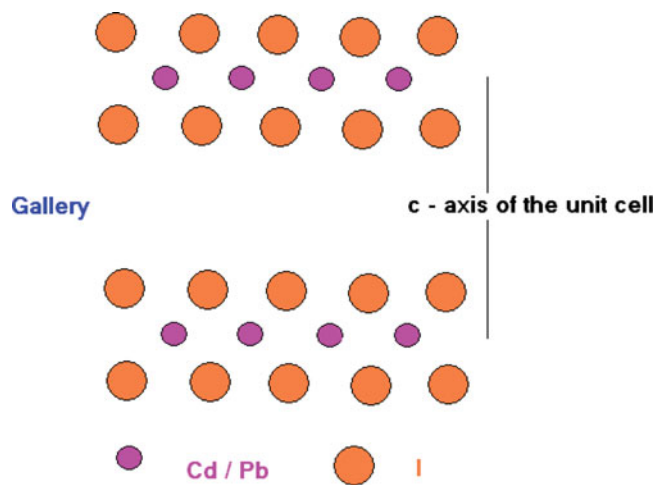


**Figure 1.** Schematic structure of layered  $MI_2$  ( $M = Pb$  and  $Cd$ ).

atoms. Both  $PbI_2$  and cadmium iodide ( $CdI_2$ ) show 0.683-nm gallery, and tetra-substituted thiuram disulfide intercalates of the two layered halides are reported in this paper.

## Results and discussion

### Infrared spectra

Table 1 shows the thioureide and C-S bond stretching frequencies observed in the sodium salts of different dithiocarbamates, corresponding  $PbI_2$  and  $CdI_2$  intercalates. The Infrared (IR) spectra show two characteristic absorptions due to  $\nu_{C-N}$  and  $\nu_{C-S}$  vibrational modes. The C-N (single bond) stretching frequency is observed in the region: 1250–1350  $cm^{-1}$  and the double bond is observed in the region: 1640–1690  $cm^{-1}$ . However, in the disulfide intercalates, vibration of C-N bond is observed in an intermediate region of wave number around 1500  $cm^{-1}$ , which is ascribed to the polar thioureide bond.<sup>24,25</sup> All the compounds show a weak band in the range of 550–700  $cm^{-1}$  corresponding to the  $\nu_{S-S}$  vibration clearly indicating the disulfide bond.<sup>26</sup>

### Electronic spectra

Representative electronic spectra of intercalates are shown in Figure 2. The pristine  $PbI_2$  is similar to golden yellow spangles, but all intercalates prepared are of fluorescent green color. Electronic spectra of  $[PbI_2]Et_2NCSS-SSCNEt_2$  and  $[CdI_2]Et_2NCSS-SSCNEt_2$  show bands at 445 nm and 433 nm respectively due to the ligand to metal charge transfer transitions.<sup>27</sup> Similar spectra were obtained for other substituted intercalates. The disulfides

with a relatively high energy lone pairs on the donating sulfur atom and a charge transfer to low lying empty metal orbitals are observed. On excitation in the wavelength range of 422–445 nm, the compounds emitted fluorescent radiation in the wave length range of 463–588 nm. In general, the cadmium intercalates emitted at higher wavelengths compared with the lead intercalates. The cadmium intercalates showed relatively weak fluorescence.

### Diffuse reflectance spectra

Representative Diffuse Reflectance Spectra are shown in Figure 3. The spectrum of  $PbI_2$  shows a characteristic band around 493 nm. The spectrum of  $[PbI_2]Et_2NCSS-SSCNEt_2$  intercalate shows a band at 441 nm due to charge transfer.<sup>27</sup> The other intercalates also showed charge transfer bands around 440 nm. Similarly, the reflectance spectra of  $CdI_2$  shows characteristic band around 385 nm. Reflectance spectra of  $[CdI_2]R'R''NCSS-SSCNR'R''$  showed charge transfer bands at 431 nm ( $R, R' = Me$ ), 435 nm ( $R, R' = Et$ ), 440 nm ( $R = Me, R' = C_6H_{11}$ ), 431 nm ( $R = Et, R' = C_6H_{11}$ ), and at 451 nm ( $R, R' = CH_2CH=CH_2$ ). The nature of substituents on the disulfides has no significant influence on the CT bands.

### Powder X-ray diffraction

Powder X-ray diffraction (XRD) patterns of lead iodide, lead iodide–tetraethylthiuram disulfide intercalate,  $[PbI_2]Et_2NCSS-SSCNEt_2$  are shown in Figure 4. The experimentally observed  $2\theta$  positions matched with the JCPDS data 07-0235, confirming the identity of  $PbI_2$ . The signal observed at  $2\theta = 12.945^\circ$  ( $d = 0.683$  nm) is the most intense signal characteristic of  $PbI_2$ . A comparison of the two patterns clearly shows appearance of a new intense signal at  $2\theta = 7.006^\circ$  ( $d = 1.260$  nm), an obvious manifestation of intercalation. The signal observed at  $12.945^\circ$  showed a reduced intensity, and shifted to lower  $2\theta = 12.177^\circ$  ( $d = 0.737$  nm). The observation is consistent with an increase in the “c”-direction of the unit cell due to the presence of a guest in gallery formed by adjacent iodine layers in the I-Pb-I “sandwich” structure.<sup>13</sup> Table 2 shows the observed XRD pattern for different intercalates with reference to the intense  $2\theta = 12.945^\circ$  signal. The XRD patterns of cadmium iodide and cadmium iodide–tetraethylthiuram disulfide intercalate are shown in Figure 5. Powder XRD of  $CdI_2$  shows characteristic signals from (001), (002), (003), and (004) planes. The experimental  $2\theta$  positions matched with the JCPDS data 84–0826, confirming the identity of the compound. The signal observed at  $2\theta = 12.945^\circ$  ( $d = 0.683$  nm) is the most intense signal characteristic of  $CdI_2$ , similar to that of  $PbI_2$ . Intercalation of  $CdI_2$  resulted in the

**Table 1.** Selected FTIR stretching frequencies.

dtc	Nadtc		$[PbI_2]R_2NCSS-SSCNR_2$			$[CdI_2]R_2NCSS-SSCNR_2$		
	$\nu_{C-N}$	$\nu_{C-S}$	$\nu_{C-N}$	$\nu_{C-S}$	$\nu_{S-S}$	$\nu_{C-N}$	$\nu_{C-S}$	$\nu_{S-S}$
$Me_2NCSS^-$ (dmdtc)	1499	970	1504	950	663	1512	959	663
$Et_2NCSS^-$ (dedtc)	1478	987	1496	980	655	1499	987	648
$(H_{11}C_6)MeNCSS^-$ (chmdtc)	1464	961	1474	956	655	1473	968	660
$(H_{11}C_6)EtNCSS^-$ (chedtc)	1450	990	1466	941	650	1479	944	649
$(H_2CCH=CH_2)_2NCSS^-$ (dadtc)	1400	999	1400	991	682	1432	926	658

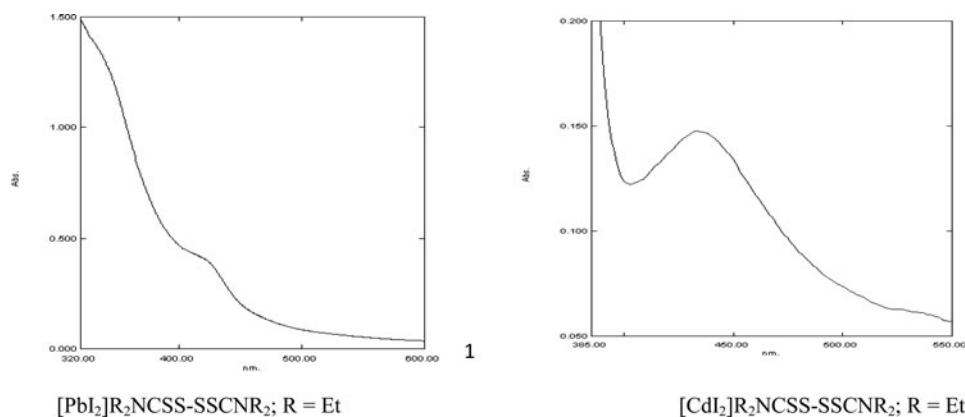
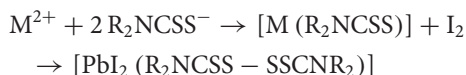


Figure 2. Representative electronic spectra of intercalates.

shifting of the (001) signal to lower  $2\theta$  value consistent with the expansion of the “c”-axis. A new intense intercalate signal appeared at  $2\theta = 9.920^\circ$  ( $d = 0.890$  nm) and a number of weak signals appeared in intercalates. The XRD signals for all the  $\text{CdI}_2$  intercalates are shown in Table 2. A close perusal of interplanar distances indicates that as the bulkiness of substituents on disulfide increases, “d” also increases. In order to differentiate between the iodinated and intercalated products,  $[\text{Pb}(\text{dedtc})_2]$  and  $[\text{Cd}(\text{dedtc})_2]$  were iodinated in  $\text{CHCl}_3$  as reported in our laboratory<sup>28</sup>:



where  $\text{M}^{2+} = \text{Pb}^{2+}/\text{Cd}^{2+}$  R = Et.

The XRD patterns of  $[\text{Pb}(\text{dedtc})_2]$  show distinct signals at  $2\theta = 12.137^\circ$  and  $9.795^\circ$ . The corresponding iodinated compound,  $[\text{PbI}_2(\text{dedtc})_2]$ , shows signals corresponding to  $2\theta = 11.808^\circ$  and at  $2\theta = 5.705^\circ$  (Figures S1 and S2; available online in Supplemental Materials). In the case of the intercalated XRD, the signals are observed at  $2\theta = 12.196^\circ$  and  $7.006^\circ$ . The observation clearly differentiates the intercalate from the iodinated

product. Similarly,  $[\text{Cd}(\text{dedtc})_2]$  shows diffracted intensity from (001) plane at  $2\theta = 11.399^\circ$  and another at  $2\theta = 9.976^\circ$ . On iodination, the signal shifts to  $2\theta = 10.892^\circ$ , which is clearly different from that of intercalate. Similar intercalation has been reported for layered double hydroxide intercalated with an anionic metallophthalocyanine.<sup>29</sup> In the present investigation, the intercalation of a thiuram disulfide into the gallery of layered  $\text{MI}_2$  is depicted as follows:

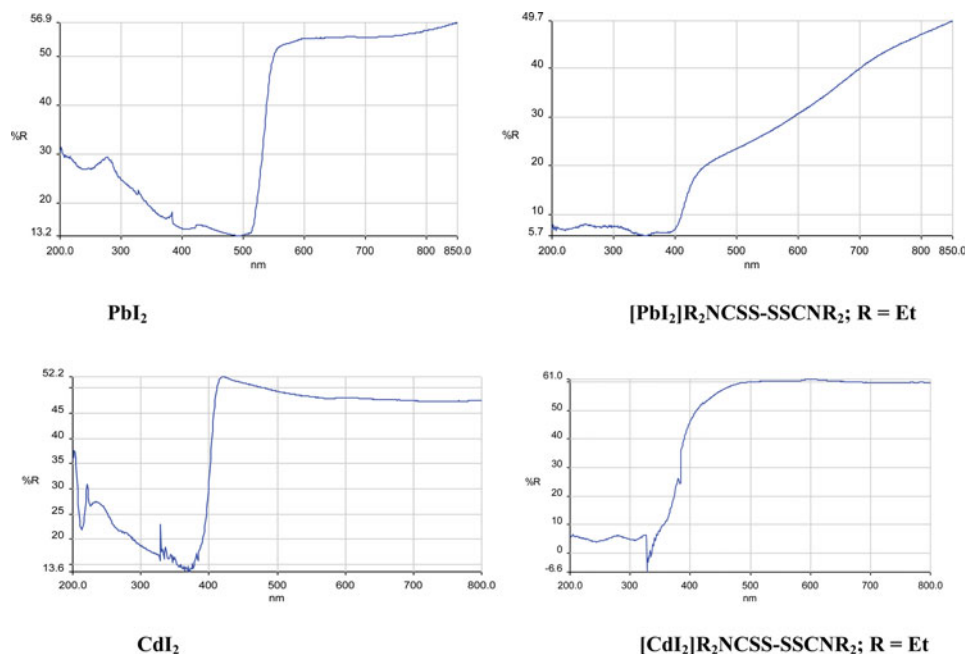
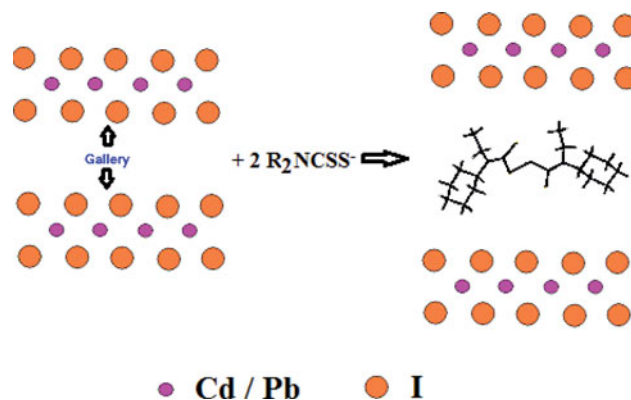


Figure 3. Diffuse reflectance spectra.

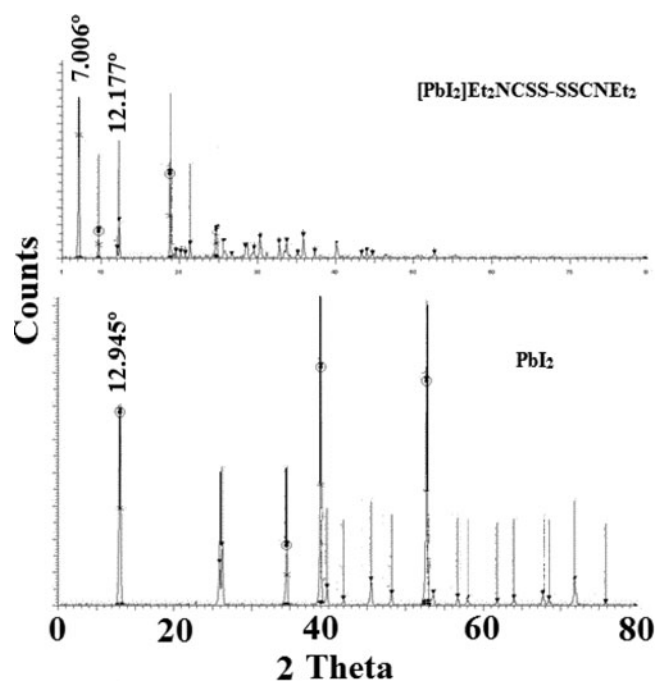


Figure 4. XRD patterns of  $\text{PbI}_2$  and  $[\text{PbI}_2]\text{Et}_2\text{NCSS-SSCNEt}_2$ .

### Thermogravimetry

The representative lead intercalates were subjected to thermal study (Figure S3; available online in Supplemental Materials).  $[\text{PbI}_2]\text{Et}_2\text{NCSS-SSCNEt}_2$  is thermally stable up to  $\sim 250^\circ\text{C}$ . Above  $250^\circ\text{C}$  the compound shows the first sign of thermal decay. A small loss in mass due to the adsorbed solvent was indicated in DTA around  $170^\circ\text{C}$ . The next significant step of decomposition is an exothermic process as indicated by the DT curve, and the decay continued up to  $305^\circ\text{C}$ . The fragment loss during the process matches in mass with that of  $\text{I}_2$ . Subsequent mass loss is also exothermic in nature and the fragment loss corresponded to the disulfide moiety,  $\text{Et}_2\text{NCSS-SSCNEt}_2$  corresponding to a mass loss of 33%. The final residue obtained around  $920^\circ\text{C}$  corresponds to  $\text{PbS}$ . The experimentally observed thermal mass losses support the proposed formula of intercalates. A similar pattern of thermal decay was observed for the cadmium intercalates. The end products could not be confirmed by XRD due to paucity of sample. The higher thermal stability associated with intercalates clearly suggests a stronger ionic interaction and a relatively difficult de-intercalation.

Table 2. Selected powder X-ray diffraction data.

Compound	M = Pb		M = Cd	
	$2\theta$ ( $^\circ$ )	d (nm)	$2\theta$ ( $^\circ$ )	d (nm)
$\text{MI}_2$	12.945	0.683	12.945	0.683
$[\text{MI}_2]\text{Me}_2\text{NCSS-SSCNEt}_2$	9.440	0.936	10.786	0.819
$[\text{MI}_2]\text{Et}_2\text{NCSS-SSCNEt}_2$	7.006	1.260	9.920	0.890
$[\text{MI}_2](\text{H}_{11}\text{C}_6)\text{MeNCSS-SSCNEt}_2$	7.123	1.240	7.097	1.244
$[\text{MI}_2](\text{H}_{11}\text{C}_6)\text{EtNCSS-SSCNEt}_2$	7.501	1.177	7.492	1.179
$[\text{MI}_2](\text{H}_5\text{C}_3)_2\text{NCSS-SSCNEt}_2$	10.124	0.873	10.443	0.846

### SEM-EDX analysis

Scanning electron microscopy (SEM) images of some selected lead and cadmium intercalates were analyzed (Figure S4; available online in Supplemental Materials). The lead intercalates are of crystalline nature and appear as rods or spheres. In particular, the diallyl-intercalate,  $[\text{PbI}_2](\text{H}_2\text{CHC}=\text{H}_2\text{C})_2\text{NCSS-SSCN}(\text{CH}_2\text{CH}=\text{CH}_2)_2$ , shows “net like structures” and  $[\text{CdI}_2](\text{H}_2\text{CHC}=\text{H}_2\text{C})_2\text{NCSS-SSCN}(\text{CH}_2\text{CH}=\text{CH}_2)_2$  are nano-crystalline with regular spherical shape. Diameter of nanoparticles are in the range of 58–75 nm. The EDX analysis of lead intercalates confirmed the presence of Pb, I, and S and are in conformity with the proposed molecular formulae of the compounds. The energy dispersive X-ray patterns of intercalates involving cadmium showed the presence of Cd, I, and S and the data are in agreement with the proposed molecular formulae of the compounds.

### HRTEM and AFM analysis

The size and morphologies of the selected intercalates of lead and cadmium dithiocarbamates are characterized by Transmission electron microscopy (TEM) analysis. High-resolution TEM (HRTEM) images are shown in Figure 6.  $[\text{PbI}_2](\text{H}_2\text{CHC}=\text{H}_2\text{C})_2\text{NCSS-SSCN}(\text{CH}_2\text{CH}=\text{CH}_2)_2$  particles are nano-rods with their diameters ranging from 13–69 nm. All the particles obtained from the remaining intercalates are also of rod shape with their diameters in the range of 13 to 130 nm. Atomic force microscopy (AFM) (Figure S5; available online in Supplemental Materials) analysis of  $[\text{PbI}_2](\text{H}_2\text{CHC}=\text{H}_2\text{C})_2\text{NCSS-SSCN}(\text{CH}_2\text{CH}=\text{CH}_2)_2$  confirmed the above observation.

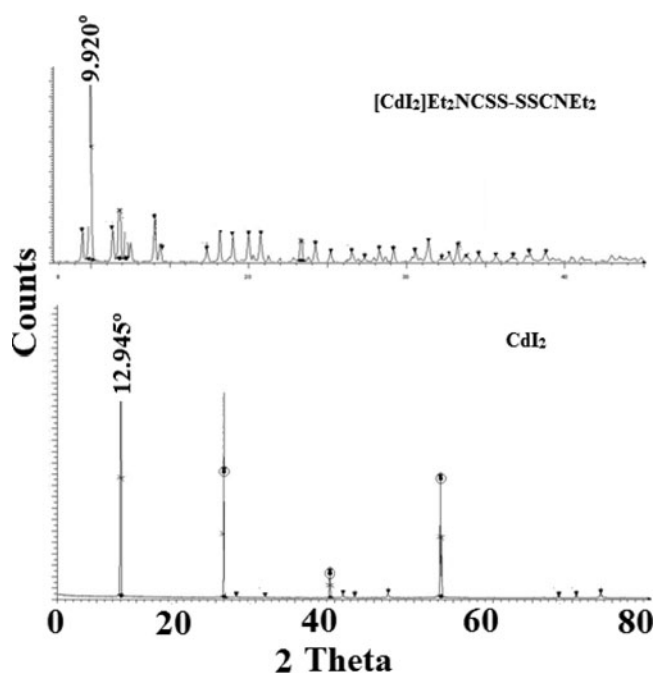


Figure 5. XRD patterns of  $\text{CdI}_2$  and  $[\text{CdI}_2]\text{Et}_2\text{NCSS-SSCNEt}_2$ .



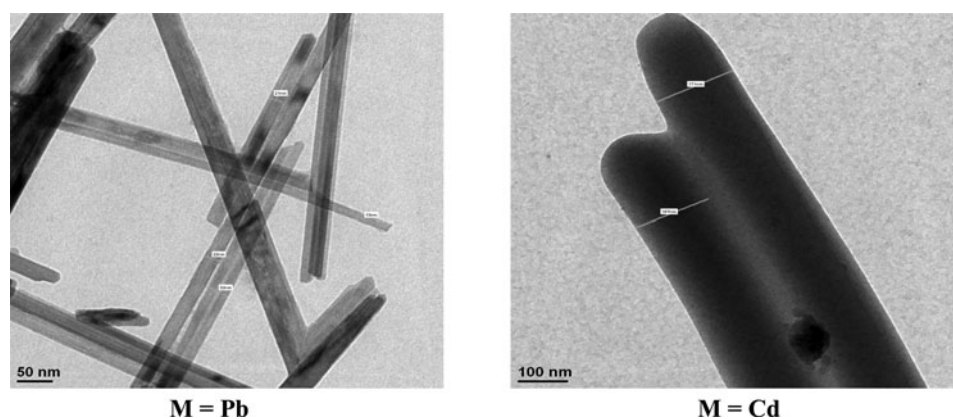
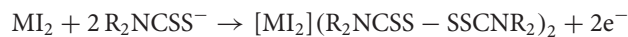


Figure 6. HRTEM images of  $[MI_2](C_3H_5)_2NCSS-SSCN(C_3H_5)_2$ .

## Conclusions

Fluorescent green  $[MI_2]R_2NCSS-SSCNR_2$  intercalates (where  $M = Pb$  or  $Cd$ ) were prepared by the reaction of binary-layered metal iodides with different dithiocarbamates in air. The neutral disulfides as oxidized dithiocarbamates are present as intercalates in the layered  $MI_2$ . Analytical data suggest 1:1 ratio of  $Pb/Cd$  to  $R_2NCSS-SSCNR_2$  in intercalates. A comparison of the thioureide stretching bands in intercalates and those observed in the sodium salts of dithiocarbamates clearly shows a significant increase in the value, and the observation is an indication of an increased contribution of thioureide form in intercalates. Therefore, the spectral data evidently support the involvement of weak interactions between polar thioureide bond and the metal centers. Electronic spectra of intercalates show bands around 440 nm due to charge transfer transitions. On excitation in the wavelength range of 422–445 nm, the compounds emitted fluorescent radiation in the wave length range of 463–588 nm. In general, the cadmium intercalates emitted at higher wavelengths compared with the lead intercalates. The cadmium intercalates showed relatively weak fluorescence. A comparison of the powder XRD patterns of  $PbI_2$  and  $[PbI_2]Et_2NCSS-SSCNET_2$  clearly shows appearance of a new intense signal at  $2\theta = 7.006^\circ$  ( $d = 1.260$  nm), an obvious manifestation of intercalation. The signal observed at  $12.945^\circ$  in  $PbI_2$  showed a reduced intensity and shifted to lower  $2\theta = 12.177^\circ$  ( $d = 0.737$  nm). The observation is consistent with an increase in the “c”-direction of the unit cell due to the presence of a guest in gallery formed by adjacent iodine layers in the “I-Pb-I sandwich” structure. The observed patterns clearly establish the fact that the disulfides insert themselves into the “gallery” in 1:1 ratio in intercalates. A similar trend was observed in the cadmium intercalates. SEM analysis of  $[PbI_2](H_2CHC=H_2C)_2NCSS-SSCN(CH_2CH=CH_2)_2$  showed it to be nano-crystalline net-like structures (58–75 nm). HRTEM analysis of  $[PbI_2](H_2CHC=H_2C)_2NCSS-SSCN(CH_2CH=CH_2)_2$  showed it to be nano-rods with their diameters in the range of 13–69 nm. AFM analysis also confirmed  $[PbI_2](H_2CHC=H_2C)_2NCSS-SSCN(CH_2CH=CH_2)_2$  particles to be of 30–69-nm diameter. Thermal decomposition of intercalates around  $900^\circ C$  led to the formation of  $PbS$  or  $CdS$ . Thermal analysis of intercalates confirmed the proposed formulae. The higher thermal stability associated with intercalates clearly suggests a stronger ionic interaction and a relatively difficult deintercalation. The intercalation process

can be summed up as intercalation of oxidized dithiocarbamate into the “galleries” of the layered  $PbI_2/CdI_2$  in the following equation:



where  $M = Pb/Cd$ ,  $R_2NCSS^- =$  dithiocarbamate anion.

## Experimental

Infrared spectra of intercalates were recorded with Avatar Nicolet FT-IR infrared spectrophotometer as KBr discs of the compounds. Electronic spectra were recorded with UV-1650 PC UV-visible spectrophotometer. Diffuse reflectance spectra were recorded on a Perkin Elmer-Lambda 35-integrated sphere spectrometer for insoluble solids. Fluorescence spectra were recorded on a Perkin Elmer Lambda LS 55 fluorescence spectrometer in dichloromethane, and Jobin Yvon Fluorolog-3-11 spectrofluorimeter was used for solid samples. To prevent any nonlinearity of fluorescence intensity, 400 nm was chosen as the excitation wavelength. Powder XRD pattern was recorded with a Bruker-D8 X-ray diffractometer using  $Cu-K\alpha$  radiation. Fixed current and potential were applied. Samples were finely powdered and mounted on glass slides. Scanning electron micrographs of the samples were recorded with JSM-6390 version 1.0 and FEI Quanta FEG 200 high-resolution scanning electron microscope. HRTEM was obtained by employing Tecnai F20, using an accelerating voltage of 200 kV. Atomic force microscopy images were taken using Park System AFM XE 100. Freshly cleaved mica substrate was used to deposit nanoparticles. The sample aliquot was left for 1 min, then washed with deionized water and left to dry for 15 min. The images were obtained by scanning mica in air in non-contact mode. Thermogravimetric analyses were carried out in nitrogen atmosphere using alumina as reference. Thermal analysis was carried out on Netzsch STA 449F3. The heating rate of the furnace was fixed at  $10^\circ C/min$  and the samples were heated up to  $1000^\circ C$  by taking approximately 5 mg of sample in a platinum crucible for each thermogravimetric experiment.

## Preparations

### Preparation of sodium salt of dithiocarbamate (Nadtc)

Amine (10 mmol) (N-ethylethanamine (de): 1.0 mL; N-methylmethanamine (dm): 0.5 mL; N-prop-2-enyl-prop-2-en-1-amine (da): 1.2 mL; N-methylcyclohexanamine (chm): 1.3 mL; N-ethylcyclohexanamine (che): 1.4 mL), and carbondisulfide (molar excess) in ethanol (5 mL) were mixed under ice-cold condition (5°C) to form yellow solution of the corresponding dithiocarbamic acid. An aqueous solution of sodium hydroxide (0.4 g; 10 mmol) was then added with continuous stirring. A pale yellow solution was obtained. Solid sodium salt was obtained by slow evaporation of ethanol solution.<sup>30–32</sup>

### Preparation of intercalated $PbI_2$ and $CdI_2$

Sodium salts of dithiocarbamates (Nadtc = sodium diethyldithiocarbamate (0.11 g; 0.5 mmol), Nadmdtc = sodium dimethyldithiocarbamate (0.07 g; 0.5 mmol), Nadaldtc = sodium diallyldithiocarbamate (0.09 g; 0.5 mmol), Nachmdtc = sodium cyclohexylmethylthiocarbamate (0.10 g; 0.5 mmol), Nachedtc = sodium cyclohexylethylthiocarbamate (0.11 g; 0.5 mmol)) were allowed to react with a solution of  $PbI_2$  (0.23; 0.5 mmol) in hot water (10 mL) and the formation of a fluorescent green precipitate was observed. The precipitate was quickly filtered, washed with hot water, and dried in air. The cadmium analogues were prepared by dissolving  $CdI_2$  (0.36 g; 1 mmol) in ethanol (10 mL) and reacting with equi-molar sodium dithiocarbamates in ethanol. The yields obtained, melting points, and elemental analyses are as follows: [ $PbI_2(dedtc)_2$ ] (1):  $C_{10}H_{20}I_2N_2PbS_4$ , Mol. Wt: 757.2; Anal. Calcd. (%): C, 15.86; H, 2.66; N, 3.70; Found: C, 15.82; H, 2.63; N, 3.67; [ $PbI_2(dmtdtc)_2$ ]· $C_2H_5OH$ · $H_2O$  (2):  $C_8H_{20}I_2N_2O_2PbS_4$ , Mol. Wt: 765.1; Anal. Calcd. (%): C, 12.56; H, 2.63; N, 3.66; Found: C, 12.52; H, 2.60; N, 3.62; [ $PbI_2(daldtc)_2$ ] (3):  $C_{14}H_{20}I_2N_2PbS_4$ , Mol. Wt: 805.2; Anal. Calcd. (%): C, 20.88; H, 2.50; N, 3.48; Found: C, 20.84; H, 2.47; N, 3.43; [ $PbI_2(chmdtc)_2$ ] (4):  $C_{16}H_{28}I_2N_2PbS_4$ , Mol. Wt: 837.3; Anal. Calcd. (%): C, 22.95; H, 3.37; N, 3.34; Found: C, 22.89; H, 3.33; N, 3.30; [ $PbI_2(chedtc)_2$ ] (5):  $C_{18}H_{32}I_2N_2PbS_4$ , Mol. Wt: 865.4; Anal. Calcd. (%): C, 24.98; H, 3.73; N, 3.24; Found: C, 24.94; H, 3.69; N, 3.20; [ $CdI_2(dedtc)_2$ ] (6):  $C_{10}H_{20}CdI_2N_2S_4$ , Mol. Wt.: 662.4; Anal. Calcd. (%): C, 18.13; H, 3.04; N, 4.23; Found: C, 18.09; H, 3.00; N, 4.20; [ $CdI_2(dmtdtc)_2$ ] (7):  $C_6H_{12}CdI_2N_2S_4$ , Mol. Wt.: 606.3; Anal. Calcd. (%): C, 11.89; H, 1.99; N, 4.62; Found: C, 11.85; H, 1.95; N, 5.59; [ $CdI_2(daldtc)_2$ ] (8):  $C_{14}H_{20}CdI_2N_2S_4$ , Mol. Wt.: 710.4; Anal. Calcd. (%): C, 23.67; H, 2.84; N, 3.94; Found: C, 23.64; H, 2.80; N, 3.90; [ $CdI_2(chmdtc)_2$ ] (9):  $C_{16}H_{28}CdI_2N_2S_4$ , Mol. Wt.: 742.5; Anal. Calcd. (%): C, 25.88; H, 3.80; N, 3.77; Found: C, 25.84; H, 3.76; N, 3.74; [ $CdI_2(chedtc)_2$ ] (10):  $C_{18}H_{32}CdI_2N_2S_4$ , Mol. Wt.: 770.6; Anal. Calcd. (%): C, 28.06; H, 4.19; N, 3.63; Found: C, 28.02, H, 4.16; N, 3.59.

### Preparation of $[MI_2(dedtc)_2]$ (where $M = Pb$ or $Cd$ )

$[M(dedtc)_2]$  (1 mmol) (where  $M = Pb$  or  $Cd$ ) was dissolved in dichloromethane, and a dilute solution of iodine (1 mmol) in chloroform (50 mL) was added drop-wise with continuous stirring over a long period of time (60 min). The precipitate

obtained was washed with dichloromethane and dried in air.

### Preparation of $[M(dedtc)_2]$ (where $M = Pb$ or $Cd$ )

Lead nitrate (0.33 g, 1 mmol)/cadmium nitrate (0.30 g, 1 mmol) were dissolved in water and an aqueous solution of sodium diethyldithiocarbamate (0.45 g, 2 mmol) in ethanol–water (1:1) was added with continuous stirring. Solid crystalline precipitates were obtained, which were washed with ethanol and dried in air, and the yield was about 80%.

## References

- Kickelbick, G. (Ed.). *Hybrid Materials, Synthesis, Characterization and Applications*; Wiley-VCH Verlag: Weinheim, Germany, 2007.
- Rath T.; Trimmel, G. *Hybrid Mater.* **2013**, *1*, 15–36.
- Kickelbick, G. *Hybrid Mater.* **2014**, *1*, 39–51.
- Kamat, P. V. *J. Am. Chem. Soc.* **2014**, *136*, 3713–3714.
- Burschka, J.; Pellet, N.; Moon, S.-J.; Humprey-Baker, R.; Gao, P.; Nazeeruddin, M. K.; Graetzel, M. *Nature* **2013**, *499*, 316–319.
- Baikie, T.; Fang, Y.; Kadro, J. M.; Schreyer, M.; Wei, F.; Mhaisalkar, S. G.; Graetzel, M.; White, T. J. *J. Mater. Chem. A* **2013**, *1*, 5628–5641.
- Stoumpos, C. C.; Malliakas, C. D.; Kanatzidis, M. G. *Inorg. Chem.* **2013**, *52*, 9019–9038.
- Wang, Y.; Gould, T.; Dobson, J. E.; Zhang, H.; Yang, H.; Yao, X.; Zhao, H. *Phys. Chem. Chem. Phys.* **2014**, *16*, 1424–1429.
- Gomez-Romero, G.; Sanchez, C. (Eds.). *Functional Hybrid Materials*; Wiley-VCH Verlag: Weinheim, Germany, **2004**.
- Subba Rao, G. V.; Shafer, M. W.; Levy, F. (Ed.). *Physics and Chemistry of Materials with Layered Structures*; Reidel: The Netherlands, **1979**.
- Gurina, G. I.; Savchenko, K. V. *J. Solid State Chem.* **2004**, *177*, 909–915.
- Gurina, G. I.; Savchenko, K. V. *J. Photochem. Photobiol. A* **1995**, *86*, 81–84.
- Mehrotra, V.; Lombardo, S.; Thompson, M. O.; Giannelis, E. P. *Phys. Rev. B* **1991**, *44*, 5786–5790.
- Glatfelter, A.; Dybowski, C.; Bai, S.; Perry, D. L. *Mater. Lett.* **2007**, *61*, 437–439.
- Novosad, S. S.; Novosad, I. S.; Goncharuk, V. E.; Kostyk, L. V. *Funct. Mater.* **2004**, *11*, 735–741.
- Matuchová, M.; Prochazková, O.; Zdanský, K.; Zavadil, J.; Maixner, J. *Mat. Sci. Forum* **2005**, *477*, 480–481.
- Wang, W.; Qiao, J.; Wang, L.; Duan, L.; Zhang, D.; Yang, W.; Qiu, Y. *Inorg. Chem.* **2007**, *46*, 10252–10260.
- Chen, W.; Wang, M.; Liu, X.; Guo, G.; Huang, J. *J. Crystal Growth Des.* **2006**, *6*, 2289–2300.
- Baibarak, M.; Baltog, I.; Lafrant, S. *Solid State Chem.* **2009**, *182*, 827–835.
- Preda, N.; Mihut, L.; Biabarac, M.; Baltog, I.; Husanu, M.; Bucur, C.; Velula, T. *Rom. J. Phys.* **2009**, *54*, 667–675.
- Savchuk, A. I.; Fediv, V. I.; Kandyba, Ye. O.; Savchuk, T. A.; Stolyarchuk, V.; Nikitin, P. I. *Mater. Sci. Eng. C* **2002**, *19*, 59–62.
- Schluter, I. Ch.; Schluter, M. *Phys. Rev. B* **1974**, *9*, 1652–1655.
- Robertson, J. *Solid State Commun.* **1978**, *26*, 791–794.
- Hogarth, G. *Prog. Inorg. Chem.* **2005**, *53*, 71–561.
- Coucovanis, D. *Prog. Inorg. Chem.* **1979**, *26*, 301–469.
- Van Wart, H. E.; Scheraga, H. A. *Proc. Natl. Acad. Sci. USA* **1986**, *83*, 3064–3067.
- Tubbs, M. R. *J. Phys. Chem. Solids* **1968**, *29*, 1191–1203.
- Thirumaran, S.; Ramalingam, K.; Bocelli, G.; Cantoni, A. *Polyhedron* **2000**, *19*, 1279–1282.
- Constantino, V. R. L.; Barbosa, C. A. S.; Bizeto, M. A.; Dias, P. M. *An. Acad. Bras. Ci.* **2000**, *72*, 45–49.
- Coucovanis, D. *Prog. Inorg. Chem.* **1970**, *11*, 233–271.
- Ramalingam, K.; Alexander, N.; Rizzoli, C. *Monatsh Chem.* **2013**, *144*, 1329–1334.
- Alexander, N.; Ramalingam, K.; Rizzoli, C. *Inorg. Chim. Acta* **2011**, *365*, 480–483.